

Exploring a possible origin of a 14 deg y-normal spin tilt at RHIC polarimeter

F. Meot

June 2015

Collider Accelerator Department
Brookhaven National Laboratory

U.S. Department of Energy

USDOE Office of Science (SC), Nuclear Physics (NP) (SC-26)

Notice: This technical note has been authored by employees of Brookhaven Science Associates, LLC under Contract No. DE-SC0012704 with the U.S. Department of Energy. The publisher by accepting the technical note for publication acknowledges that the United States Government retains a non-exclusive, paid-up, irrevocable, world-wide license to publish or reproduce the published form of this technical note, or allow others to do so, for United States Government purposes.

DISCLAIMER

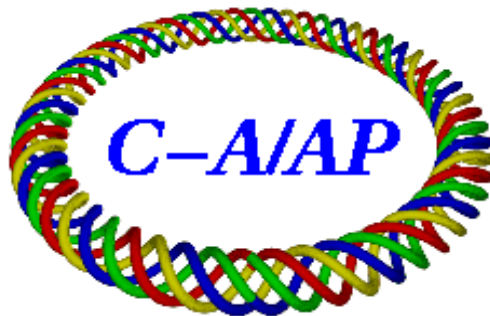
This report was prepared as an account of work sponsored by an agency of the United States Government. Neither the United States Government nor any agency thereof, nor any of their employees, nor any of their contractors, subcontractors, or their employees, makes any warranty, express or implied, or assumes any legal liability or responsibility for the accuracy, completeness, or any third party's use or the results of such use of any information, apparatus, product, or process disclosed, or represents that its use would not infringe privately owned rights. Reference herein to any specific commercial product, process, or service by trade name, trademark, manufacturer, or otherwise, does not necessarily constitute or imply its endorsement, recommendation, or favoring by the United States Government or any agency thereof or its contractors or subcontractors. The views and opinions of authors expressed herein do not necessarily state or reflect those of the United States Government or any agency thereof.

C-A/AP/538

June 2015

**Exploring a possible origin of a 14 deg y-normal spin \vec{n}_0 tilt
at RHIC polarimeter**

F. Meot, H. Huang



**Collider-Accelerator Department
Brookhaven National Laboratory
Upton, NY 11973**

**U.S. Department of Energy
Office of Science, Office of Nuclear Physics**

Notice: This document has been authorized by employees of Brookhaven Science Associates, LLC under Contract No. DE-SC0012704 with the U.S. Department of Energy. The United States Government retains a non-exclusive, paid-up, irrevocable, world-wide license to publish or reproduce the published form of this document, or allow others to do so, for United States Government purposes.

Exploring a possible origin of a 14 deg y-normal spin \vec{n}_0 tilt at RHIC polarimeter.

F. Méot, H. Huang

BNL C-AD, Upton, LI, NY 11973

June 2015

Abstract

A possible origin of a 14 deg y-normal spin \vec{n}_0 tilt at the polarimeter is in snake angle defects. This possible cause is investigated by scanning the snake axis angle μ , and the spin rotation angle at the snake, ϕ , in the vicinity of their nominal values.

Tech Note C-A/AP/538

Contents

| | | |
|----------|--|-----------|
| 1 | Introduction | 3 |
| 2 | Working hypotheses | 3 |
| 3 | “Run 13 optics” | 3 |
| 3.1 | Case of zero vertical orbit | 3 |
| 3.2 | Case of a 0.13 mm <i>rms</i> vertical orbit | 6 |
| 3.3 | Case of a 0.26 mm <i>rms</i> vertical orbit | 7 |
| 4 | Case of “pp11v7 optics” | 8 |
| 4.1 | Case of vertical separation bumps at all IPs | 9 |
| 4.2 | Case of zeroed vertical bumps at IPs 6, 8 | 12 |
| 5 | Summary | 13 |

1 Introduction

In recent analysis of run13 p-carbon polarimeter measurements, it was found that spin angle was significantly tilted away from vertical. The measurements showed that this was the case at both injection and store of 255 GeV. A possible origin of a 14 deg y-normal spin \vec{n}_0 tilt at the polarimeter is in snake angle defects. This possible cause is investigated by scanning the snake axis angle μ , and the spin rotation angle at the snake, ϕ , in the vicinity of their nominal values.

2 Working hypotheses

- Blue ring is considered, The origin of the Zgoubi input data file is from translation of the MADX “blue holy lattice”. It also happens to be the very file used for earlier spin tracking studies which can be referred to if necessary, in particular, “Effect of snake rotation angle error on spin transmission through 411-Qy”, June 2011 spin meeting.
- 255 GeV store is considered, with two different optics, called “Run 13” or “pp11v7” in the following.
- The game in this study consists in changing (i) the orientation of the snake axes, which are contained in the plane of the ring with μ_1, μ_2 their angle to the beam axis, and (ii) the spin rotation angle at the snakes, ϕ_1, ϕ_2 , within the following limits :
 - snake axes are maintained at constant $\Delta\mu = 90$ degrees from one another (the design value)
 - ϕ_1 and ϕ_2 are moved away from the 180 degrees design value independently from one another.
- For any (μ, ϕ) arrangement, just one set of random orbit defects is run : it remains to be confirmed that this does give a correct idea of the value of the y-normal tilt of spin \vec{n}_0 around the ring (by y-normal, it is meant a rotation with axis contained in the horizontal plane, which moves \vec{n}_0 away from the vertical).

Method :

A fitting procedure is used to find \vec{n}_0 from the lattice once the snake axis angles μ_1, μ_2 or the snake angles ϕ_1, ϕ_2 have been moved.

3 “Run 13 optics”

The optics of concern is summarized in Figs. 1-4. In these simulations a vertical orbit may be considered, in that case it is scaled from that displayed in Fig. 1; the horizontal orbit is scaled similarly, with the same *rms* value.

3.1 Case of zero vertical orbit

In these μ and ϕ scans, the orientation of snake 1 axis takes the values $\mu_1 : -90 \rightarrow +90$ deg. (step 45 deg.) whereas snake 2 axis takes the values $\mu_2 = \mu_1 - 90$ deg.

The spin rotation angle ϕ takes its values between 160 and 200 deg., for both snakes.

This generates the set of curves below.

**"Run 13" optics,
including vertical orbit (corrected from 29th harmonic)**

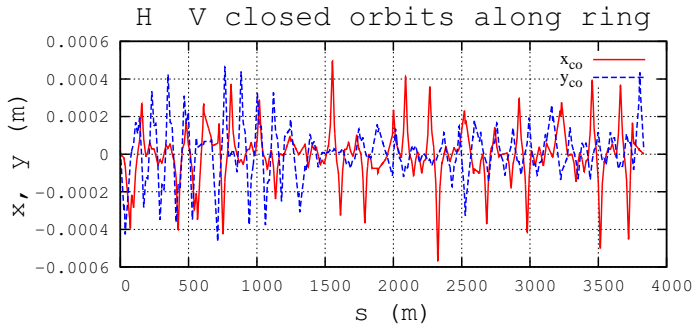


Figure 1: H and V orbits. The *rms* value of the vertical orbit in the arcs is $25\mu\text{m}$.

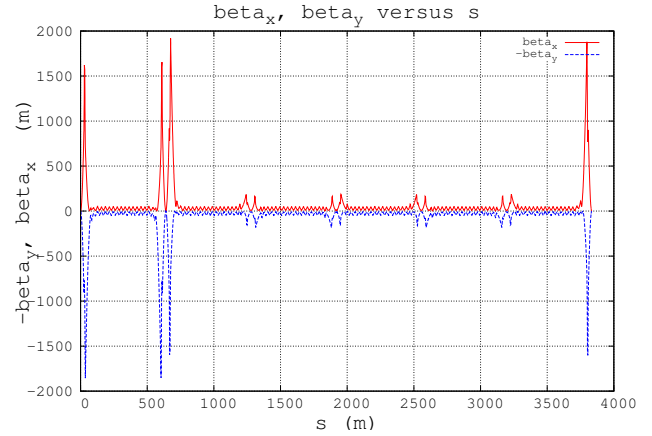


Figure 2: Horizontal and vertical optical functions.

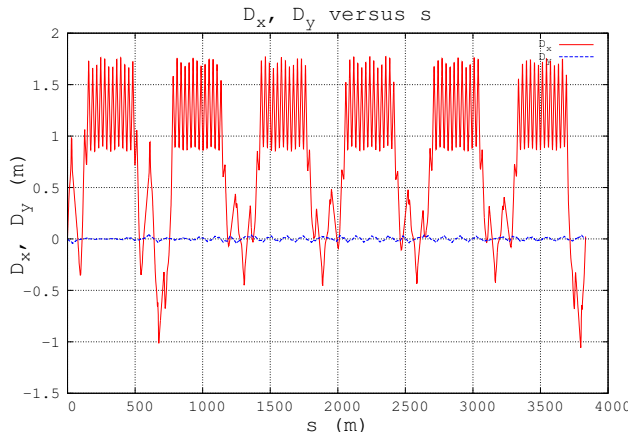


Figure 3: Horizontal and vertical dispersions.

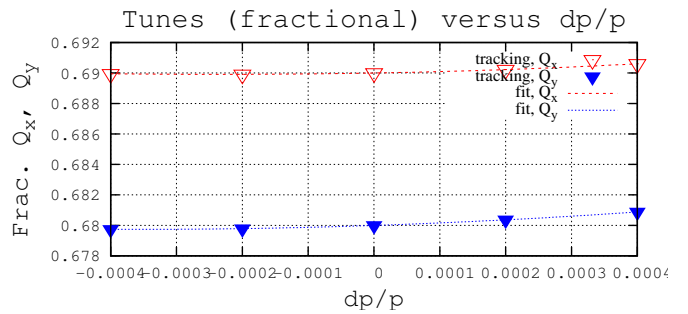
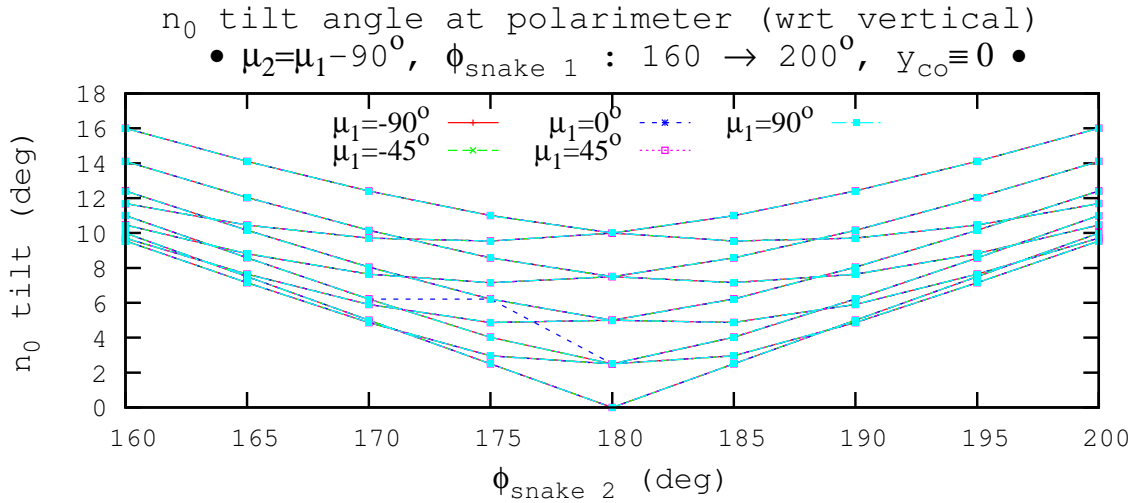


Figure 4: Momentum dependence of tunes, and matching polynomials $Q(\delta) = Q_0 + Q'\delta + Q''\delta^2 + Q'''\delta^3$.

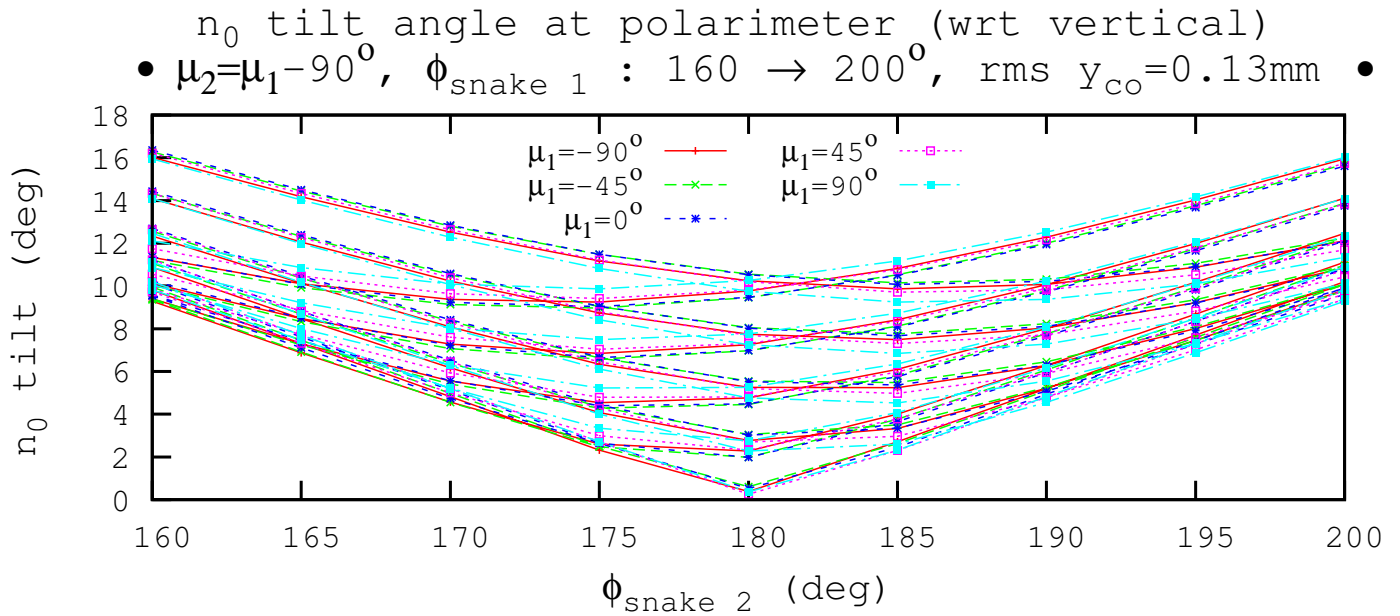
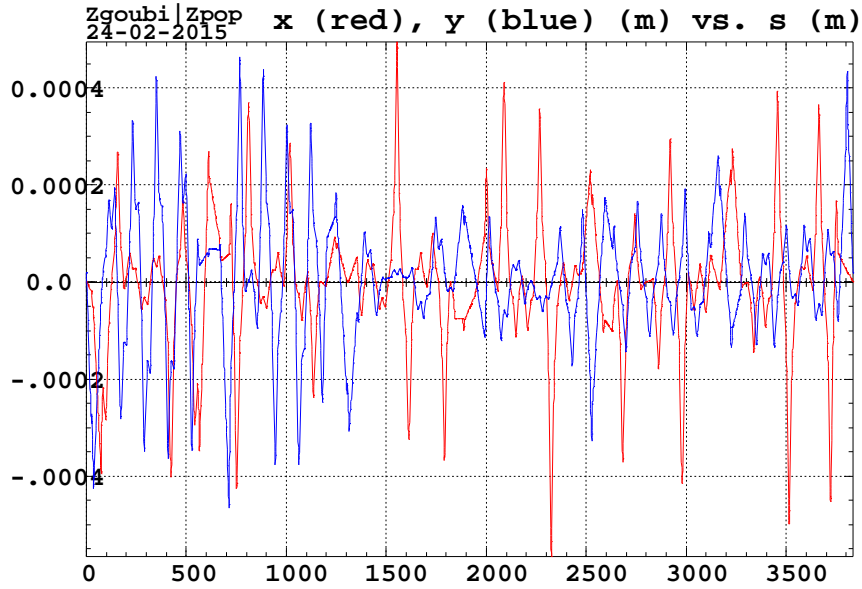


Details of some of the numerical values in the figure above :

| mu_2+90 | | | ----- @ clock6 ----- | | | ----- angle to y axis ----- | | |
|---------|-------|-------|----------------------|---------|--------|-----------------------------|----------|-----------|
| =mu_1 | phi_1 | phi_2 | n_0_1 | n_0_x | n_0_y | @clock6 | @PJET | @Polarmtr |
| deg. | deg. | deg. | | | | deg. | deg. | deg. |
| 45. | 170. | 170. | -0.0354 | 0.0965 | 0.9948 | 5.8372 | 171.9635 | 171.9635 |
| 45. | 170. | 180. | -0.0838 | 0.0244 | 0.9963 | 4.9328 | 175.0065 | 175.0065 |
| 45. | 170. | 190. | -0.1314 | -0.0479 | 0.9901 | 8.0593 | 174.1027 | 174.1027 |
| 45. | 180. | 170. | 0.0483 | 0.0726 | 0.9963 | 4.9328 | 174.9980 | 174.9980 |
| 45. | 180. | 180. | -0.0001 | 0. | 1. | 0. | 180. | 180.0000 |
| 45. | 180. | 190. | -0.0482 | -0.0726 | 0.9963 | 4.9328 | 175.0006 | 175.0006 |
| 45. | 190. | 170. | 0.1314 | 0.0481 | 0.9901 | 8.0593 | 174.0938 | 174.0938 |
| 45. | 190. | 180. | 0.0837 | -0.0244 | 0.9962 | 4.9873 | 175.0011 | 175.0011 |
| 45. | 190. | 190. | 0.0353 | -0.0965 | 0.9947 | 5.8834 | 171.9607 | 171.9607 |
| 45. | 160. | 160. | -0.0695 | 0.1904 | 0.9793 | 11.6897 | 163.9927 | 163.9927 |
| 45. | 160. | 165. | -0.0942 | 0.1553 | 0.9835 | 10.4363 | 165.8937 | 165.8937 |
| 45. | 160. | 170. | -0.1186 | 0.1198 | 0.9857 | 9.7083 | 167.5955 | 167.5955 |
| 45. | 160. | 175. | -0.1428 | 0.0844 | 0.9862 | 9.5390 | 169.0043 | 169.0043 |
| 45. | 160. | 180. | -0.1667 | 0.0486 | 0.9849 | 9.9568 | 170.0015 | 170.0015 |
| 45. | 160. | 185. | -0.1905 | 0.0128 | 0.9817 | 10.9696 | 170.4618 | 170.4618 |
| 45. | 160. | 190. | -0.2137 | -0.0230 | 0.9765 | 12.4344 | 170.2988 | 170.2988 |
| 45. | 160. | 195. | -0.2366 | -0.0588 | 0.9699 | 14.0989 | 169.5475 | 169.5475 |
| 45. | 160. | 200. | -0.2588 | -0.0946 | 0.9612 | 16.0056 | 168.3069 | 168.3069 |

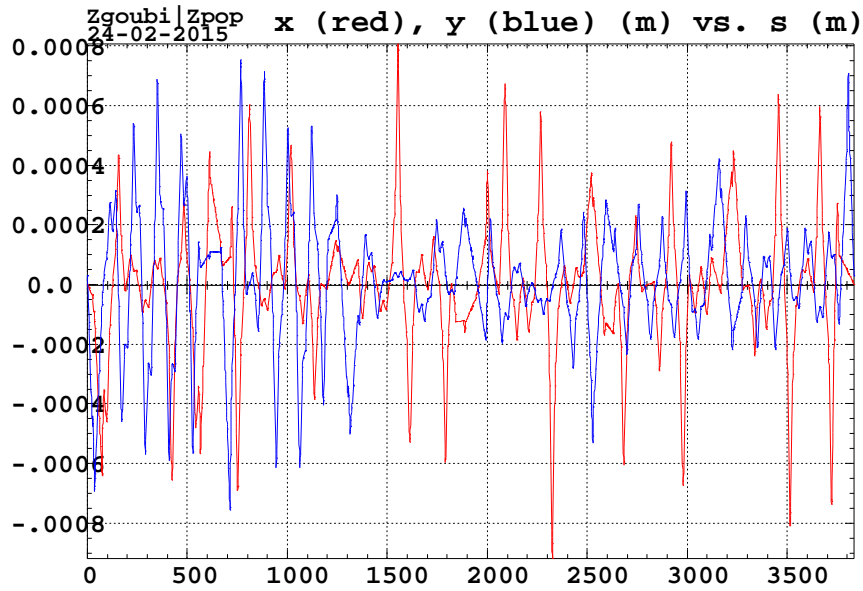
3.2 Case of a 0.13 mm rms vertical orbit

In these μ and ϕ scans, the vertical orbit is scaled from that displayed in Fig. 1, with an *rms* value of 0.13 mm. The *rms* horizontal orbit is 0.13 mm as well.



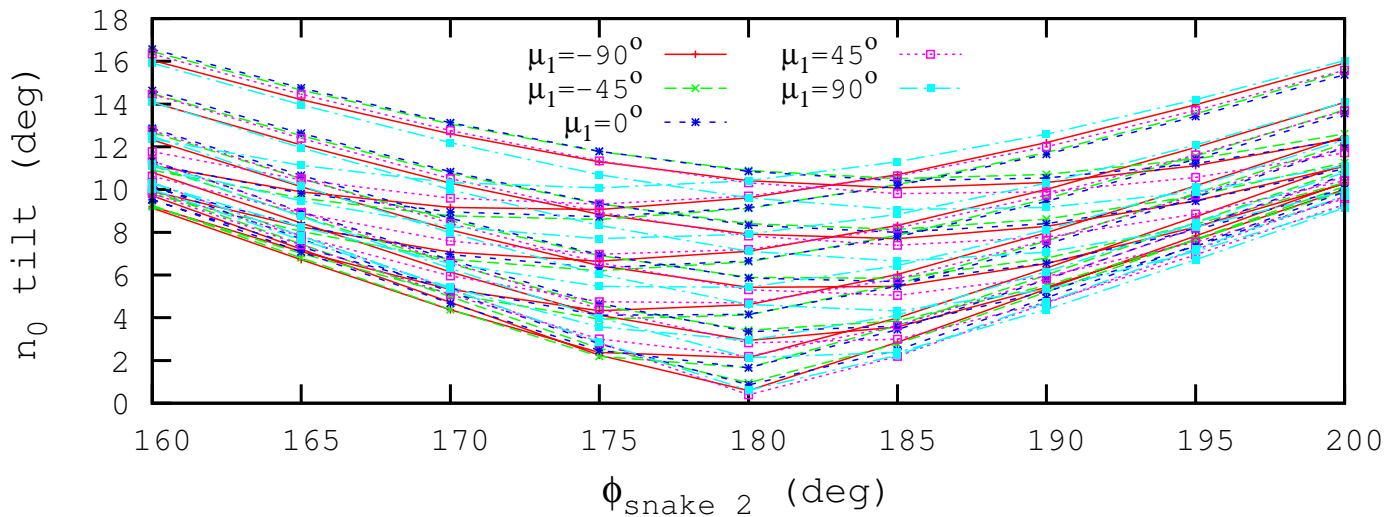
3.3 Case of a 0.26 mm rms vertical orbit

In these μ and ϕ scans, the vertical orbit is scaled from that displayed in Fig. 1, with an *rms* value of 0.26 mm. The *rms* horizontal orbit is 0.26 mm as well.



n_0 tilt angle at polarimeter (wrt vertical)

- $\mu_2 = \mu_1 - 90^\circ$, $\phi_{\text{snake } 1} : 160 \rightarrow 200^\circ$, rms $y_{\text{co}} = 0.26\text{mm}$ •



4 Case of “pp11v7 optics”

This optics is that of the ramp and includes vertical separation bumps at IPs. Although this is not the conditions for the polarization measurements addressed here, the interest is to assess a possible effect of such bumps.

Working conditions in this “pp11v7” style optics are displayed in Figs. 5-8. They are the same as in the spin tracking simulations presented at the Nov. 2011 spin meeting, which can be referred to for details.

“pp11v7 optics”, including vertical separation bumps at IPs

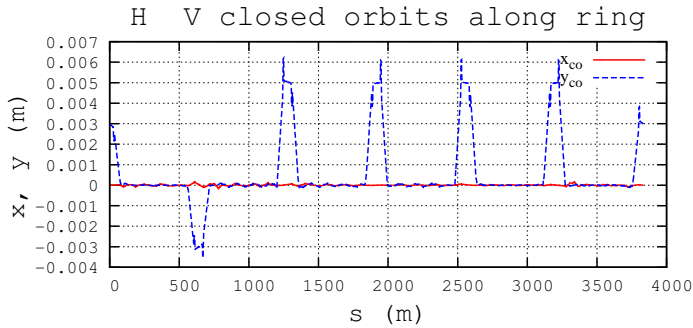


Figure 5: H and V orbits. The rms value of the vertical orbit in the arcs is $25\mu\text{m}$.

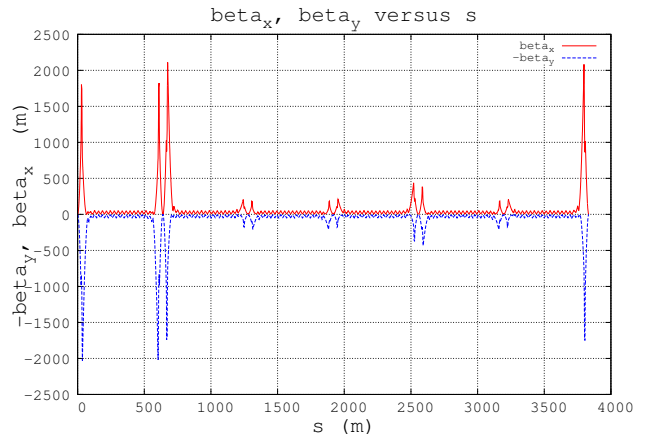


Figure 6: Horizontal and vertical optical functions.

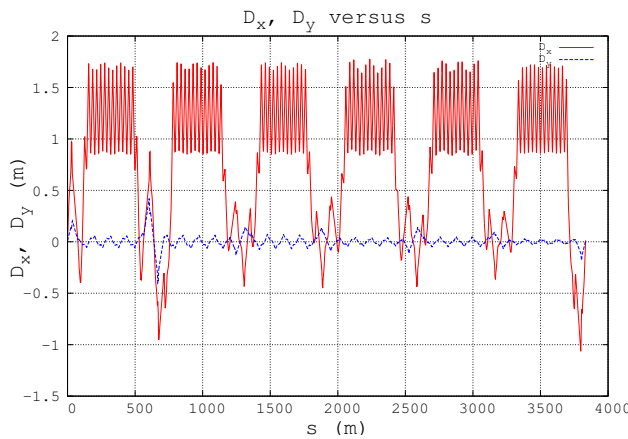


Figure 7: Horizontal and vertical dispersions.

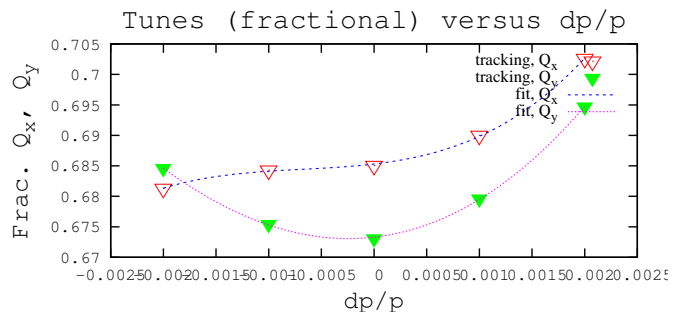


Figure 8: Momentum dependence of tunes, and matching polynomials $Q(\delta) = Q_0 + Q'\delta + Q''\delta^2 + Q'''\delta^3$.

Horizontal : $Q_x = 0.6853, Q'_x = 2.037$

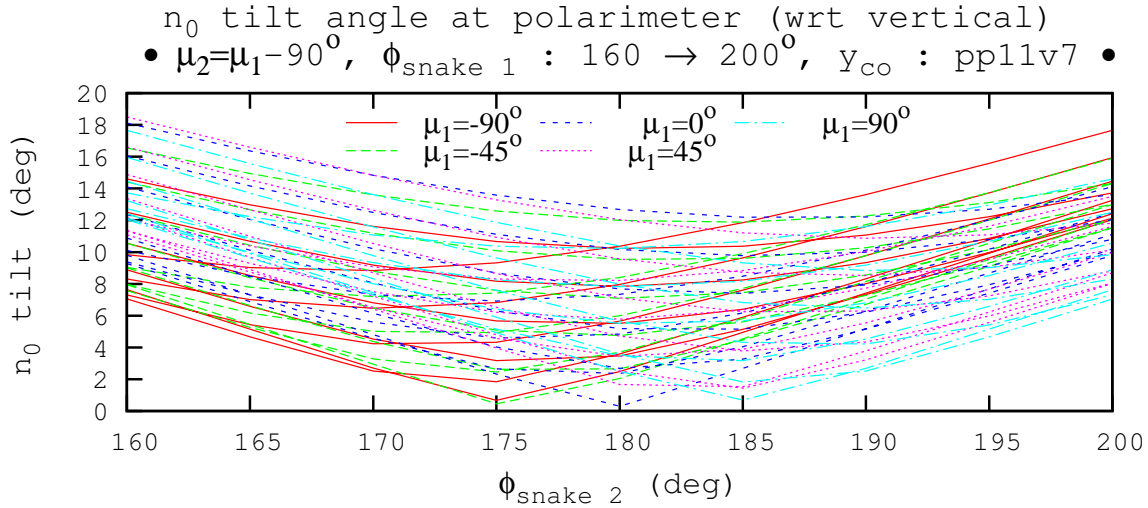
Vertical : $Q_y = 0.6732, Q'_y = 1.950$

4.1 Case of vertical separation bumps at all IPs

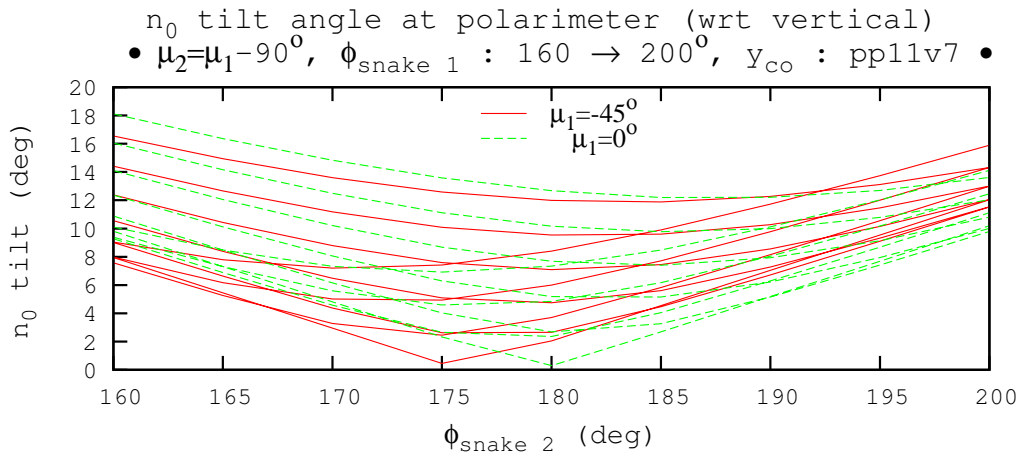
In these μ and ϕ scans, the orientation of snake 1 axis takes the values $\mu_1 : -90 \rightarrow +90$ deg. (step 45 deg.) whereas snake 2 axis angle takes the values $\mu_2 = \mu_1 - 90$ deg.

The spin rotation angle ϕ takes its values between 160 and 200 deg., for both snakes.

This generates the set of curves below.



The graph below is an excerpt of the one above, for clarification.



The table below gives details regarding the curves displayed in the previous figures.

| mu_2+90 | | | ----- @ clock6 ----- | | | ----- angle to y axis ----- | | |
|---------|-------|-------|----------------------|---------|--------|-----------------------------|----------|-----------|
| =mu_1 | phi_1 | phi_2 | n_0_1 | n_0_x | n_0_y | @clock6 | @PJET | @Polarmtr |
| deg. | deg. | deg. | | | | deg. | deg. | deg. |
| 45. | 170. | 170. | -0.0308 | 0.0914 | 0.9953 | 5.5521 | 172.2901 | 169.4557 |
| 45. | 170. | 180. | -0.0789 | 0.0191 | 0.9965 | 4.7653 | 175.1204 | 172.8754 |
| 45. | 170. | 190. | -0.1268 | -0.0533 | 0.9904 | 7.9577 | 173.8732 | 173.7120 |
| 45. | 180. | 170. | 0.0528 | 0.0674 | 0.9963 | 4.9328 | 175.3964 | 172.7744 |
| 45. | 180. | 180. | 0.0047 | -0.0052 | 1. | 0. | 179.6053 | 177.4910 |
| 45. | 180. | 190. | -0.0437 | -0.0778 | 0.9960 | 5.0945 | 174.6010 | 176.7851 |
| 45. | 190. | 170. | 0.1360 | 0.0427 | 0.9899 | 8.1596 | 174.3120 | 173.4801 |
| 45. | 190. | 180. | 0.0884 | -0.0296 | 0.9956 | 5.4039 | 174.8511 | 176.5602 |
| 45. | 190. | 190. | 0.0400 | -0.1020 | 0.9941 | 6.2406 | 171.6190 | 174.4574 |
| 0. | 170. | 170. | 0.0452 | 0.0853 | 0.9953 | 5.5521 | 172.1957 | 169.7911 |
| 0. | 170. | 180. | -0.0401 | 0.0684 | 0.9969 | 4.5326 | 175.1808 | 172.3233 |
| 0. | 170. | 190. | -0.1250 | 0.0511 | 0.9909 | 7.7157 | 174.0857 | 172.0715 |
| 0. | 180. | 170. | 0.0872 | 0.0092 | 0.9962 | 4.9873 | 175.2045 | 173.8502 |
| 0. | 180. | 180. | 0.0018 | -0.0081 | 1. | 0. | 179.7569 | 177.3158 |
| 0. | 180. | 190. | -0.0836 | -0.0253 | 0.9960 | 5.0945 | 174.7913 | 174.8439 |
| 0. | 190. | 170. | 0.1285 | -0.0671 | 0.9894 | 8.3566 | 174.1230 | 175.4307 |
| 0. | 190. | 180. | 0.0435 | -0.0844 | 0.9956 | 5.4039 | 174.8045 | 177.6496 |
| 0. | 190. | 190. | -0.0416 | -0.1014 | 0.9941 | 6.2406 | 171.7121 | 173.7038 |

Tilt angle between \vec{n}_0 (PJET) and \vec{n}_0 (Polarimeter)

PJET and polarimeter are at respectively 1917.39376 m, 1988.53985 m (see next two figures), 71 m distant from one another. In addition,

- PJET is on the y_{co} -plateau,
- the polarimeter is at the downstream end of the y_{co} bump,

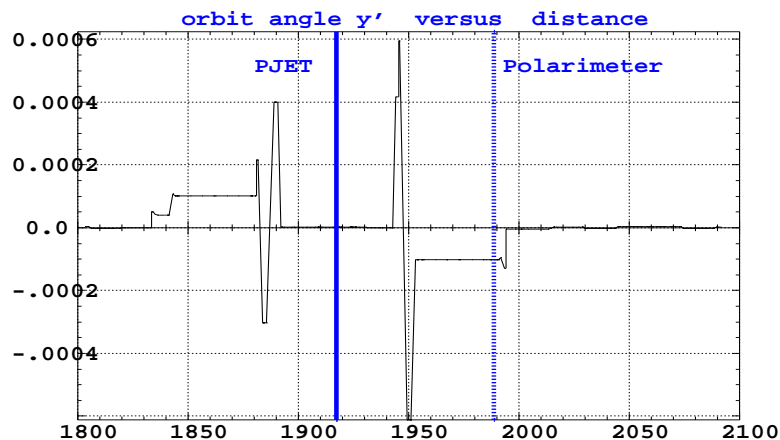
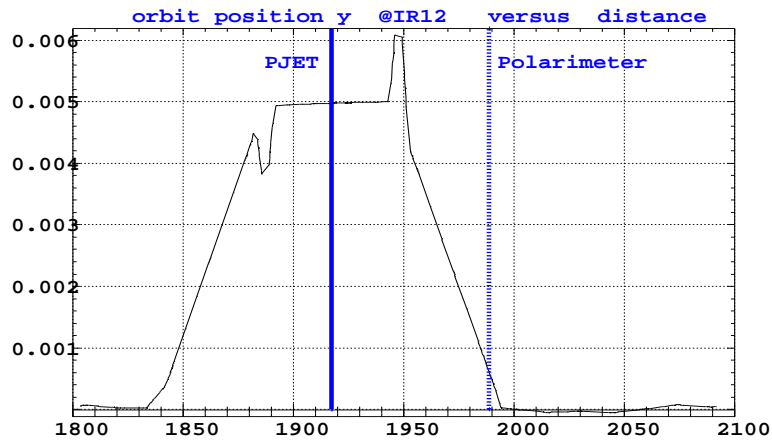
This is schemed in the two figures below : the first one shows the orbit amplitude, the second one shows the orbit angle, as a function of the distance along the ring.

Due to the vertical orbit, \vec{n}_0 undergoes a y-tilt which amounts to the integrated $G\gamma\alpha$.

From the tracking, the values of concern are as follows :

- the relative vertical orbit deviation between PJET and polarimeter is (ramp optics) $\alpha \approx 0.1$ mrad, $G\gamma\alpha \approx 49$ mrad = 2.8 deg, not far from the 2.1 deg as of the tracking for $\mu_1 = -\mu_2 = 45$ deg, $\phi_1 = \phi_2 = 180$ deg, previous page.

Scaling down to actual beam separation during store of about half less, i.e., $\alpha \approx 0.1$ mrad \rightarrow 0.05 mrad, the result is half as much, namely a ~ 1.4 deg spin tilt difference between PJET and polarimeter.



4.2 Case of zeroed vertical bumps at IPs 6, 8

Compared to the previous section the vertical bumps at IPs 6, 8 are zeroed here, figure below, so corresponding to collision conditions.

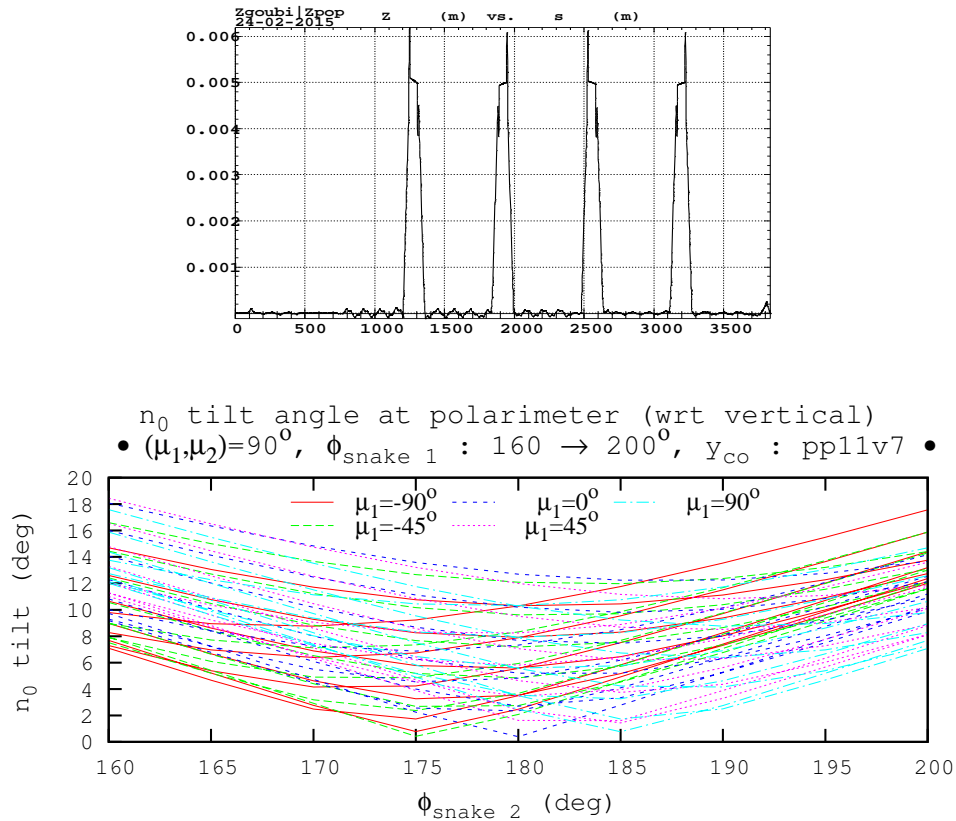
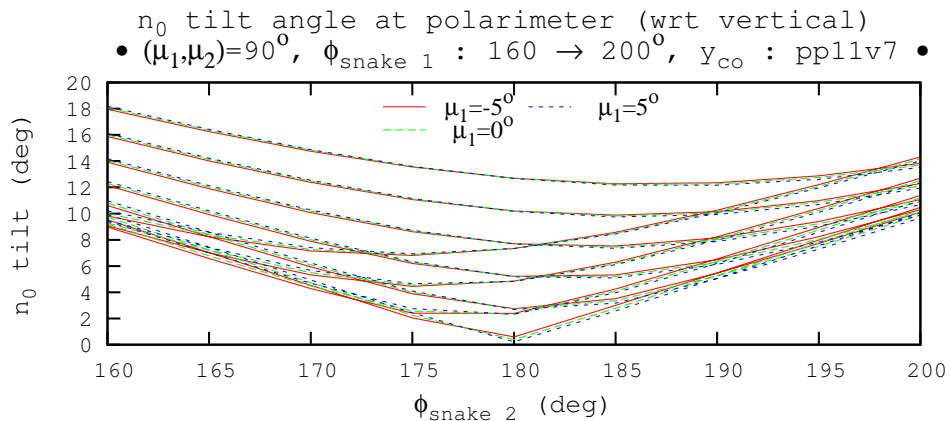


Figure below : previous case limited to μ₁ = 0, ± 5 deg.



5 Summary

Assuming correct orientation of the spin precession axes, +45 and -45 deg at snake 1, 2 respectively, the following is learned from these snake axis and spin angle scans :

- In the presence of the vertical separation bumps, a ± 10 deg. error on the snake angles ϕ_1, ϕ_2 may entail ~ 11 deg. y^\perp -tilt of spin \vec{n}_0 at the polarimeter (see page 10).
- In the absence of the separation bumps the effect is ~ 8 deg (see page 5).
- A defect of ± 5 deg in the orientation of the spin precession axis (see page 12) marginally impacts on what precedes.